40th AIAA/ASME/SAE/ASEE Joint Propulsion Conference and Exhibit
11 - 14 July 2004, Fort Lauderdale, Florida

AIAA 2004-3781

Boundary Conditions for a 2-D Hybrid Stationary Plasma Thruster Model

Justin Koo*, Michael Keidar†, and Iain Boyd‡
University of Michigan, Ann Arbor, Michigan, 48104

A 1-D anode region model is coupled to a 2-D axisymmetric hybrid PIC-MCC Hall thruster model. This anode region model is based on the premise that a sufficient presheath exists to support a stable sheath on the interior surfaces of the thruster near the anode. In practice, the ion distribution function is evaluated in the anode region to evaluate whether the generalized analytic Bohm criterion is satisfied and a simple linear feedback controller is used to make appropriate corrections to the potential field. The linear feedback controller achieves only rough convergence to oscillatory anode region potential configurations; nonetheless, these configurations can still be characterized by their mean voltage. For anode electron energies of 1 eV and 3 eV, the resulting mean anode region voltage corrections are 4 V and 15 V, respectively. Since physical mechanisms not simulated in this model are known to contribute to the formation of a stable anode presheath, these estimated mean anode region voltage corrections are believed to represent reasonable upper bounds on the actual anode region potential drop. The use of these boundary conditions in the 2-D hybrid model marginally reduces the thrust generated by the simulation.

Nomenclature

VAL	=	Virtual Anode Line
VCL	=	Virtual Cathode Line
λ	=	Magnetic Field Streamfunction
B	=	Magnetic Field
k_B	=	Boltzmann Constant
e	=	Electron Charge
M	=	Atomic Mass of Xenon
m	=	Electron Mass
ϕ^*	=	Thermalized Potential
j_e	=	Electron Current
j_i	=	Ion Current
μ_e	=	Transverse Magnetic Field Electron Mobility
$\omega_{B,e}$	=	Electron Cyclotron Frequency
g(v)	=	Normalized Ion Distribution Function
ν_{mom}	=	Electron Momentum Transfer Frequency
ν_{loss}	=	Electron Energy Loss Frequency
k_i	=	Neutral Ionization Rate
n_e	=	Plasma Density
n_a	=	Neutral Density
u_i	=	Ion Velocity
ε	=	Mean Electron Energy

I. Introduction

EXPERMENTAL study of Hall thrusters has far outpaced the computational study of these devices in the decades since their introduction; however, interest remains in the development of robust, accurate, and efficient Hall thruster codes. Many new computational models of the plasma properties inside Hall thrusters have been

* Graduate Student, Department of Aerospace Engineering, kooj@engin.umich.edu, Student Member AIAA.
† Research Scientist, Department of Aerospace Engineering, Member AIAA.
‡ Professor, Department of Aerospace Engineering, Associate Fellow AIAA.

developed recently. They range from 1-D and 2-D steady-state models such as those by Keidar et al.[i], Ahedo et al.[ii], to 2-D fluid models by Roy and Pandey[iii], to full 1-D and 2-D time dependent models by Komurasaki and Arakawa[iv], Fife[v], Boeuf and Garrigues[vi], and, most recently, by Hagelaar et al.[vii] and others. These computational models have reached a stage of refinement where, with a priori knowledge of a particular experimental flow condition, a reasonably representative computational solution can be achieved in a matter of hours.

As part of our continued development of a robust Hall thruster model, this paper studies the dependence of a particular model on anode boundary conditions. In particular, the presence of a presheath is considered in the anode region. This anode region model provides potential corrections to the main simulation region of a 2-D axisymmetric hybrid PIC-MCC model of the acceleration channel and near-field of a dielectric wall-type Hall thruster.

II. Physical Motivation

An electric sheath is expected to form near the anode face dependent on the operational conditions. This implies that there is some net ion flux towards the anode (backwards relative to the main discharge).[viii] The ion backflux constitutes the necessary condition for the existence of a stable anode sheath.[i] Physically, it is possible for a pressure gradient, a potential gradient, or some combination of these gradients to drive this ion backflow. Since the ions are assumed to be collisionless in the model of Koo[ix], only the potential gradient can be modeled with the existing code.

III. Implementation

In this numerical simulation, two distinct potential models are used in two distinct regions. The "Hall region", between the VAL (labeled Anode Line) and the VCL (labeled Cathode Line), uses a 1-D Ohm's law formulation to evaluate the potential field. The "Anode region", between the Anode and the VAL, uses an separate anode region model to calculate the potential field. These two adjacent regions are coupled to each other in the simulation. In particular, the ion distribution generated in the Hall region is used in the Anode region while the Anode region provides a correction to the total potential drop used in the Hall region.

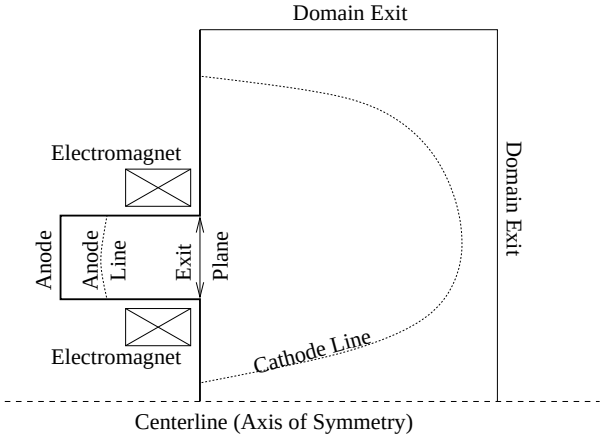

Figure 1. Hall Thruster Schematic

A. Computational Model

This model provides a 2-D axisymmetric hybrid PIC-MCC description of the acceleration channel and near-field of a dielectric wall-type Hall thruster[ix]. Plasma potential in the Hall region is calculated using a 1-D Ohm's Law formulation and plasma potential in the Anode region is calculated using an anode region model. It is based on a quasi-neutral plasma description where collisionless heavy particles (Xe and Xe^+) are treated with a PIC-MCC model. The electron fluid is modeled with a 1-D electron energy model.

An SPT-100 type field configuration is calculated using a Poisson solver ($\nabla^2 B = 0$) with channel wall boundary conditions derived from experimental sources. Magnetic field lines are used to formulate the 1-D Ohm's Law and 1-D electron energy equations.

1-D Ohm's Law Formulation (Hall Region)

Through the use of the concept of thermalized pressure, first introduced by Morozov[x], it is possible to reduce the 2-D electrostatic field calculation into a 1-D Ohm's Law formulation. This formulation is based on the assumption that there is no net buildup of charge throughout the domain and requires the sum of the electron and ion currents to balance throughout the domain as follows:

$$\begin{aligned} I_T &= \int_S j_e \partial S + \int_S j_i \partial S \\ &= \int_S e n_e \mu_e r B \left(-\frac{\partial \phi^*}{\partial \lambda} - \left[\ln\left(\frac{n_e}{n^*}\right) - 1 \right] \frac{k_B}{e} \frac{\partial T_e}{\partial \lambda} \right) \partial S \\ &\quad + \int_S e n_e u_i \partial S \end{aligned}$$

This equation is summed from the VAL to the VCL and a closed form solution for the total current can be derived. Once the total current is known, the derivative of the thermalized potential can be calculated directly and a full thermalized potential can be constructed. The thermalized potential is then extrapolated along field lines through the Hall region and the electrostatic potential is recovered. The VAL potential is updated continuously based on the results of the anode region model.

Anode Model Formulation (Anode Region)

The potential field near the anode is calculated based on the requirements that the ion distribution near the anode satisfies the generalized analytic Bohm criterion. Further description will be provided in the next section of this paper.

The transverse magnetic field electron mobility is needed for calculation of the electrostatic field. To ensure that the electron mobility does not drop catastrophically in regions of neutral depletion, the electron momentum transfer frequency is supplemented by a Bohm-type correction suggested by Fife[v]. This leads to the following term for the electron momentum transfer frequency:

$$\nu_{mom} = \nu_{neutrals} + \nu_{bohm}$$

where,

$$\nu_{neutrals} = 2.5 * 10^{-13} n_a$$

$$\nu_{bohm} = \alpha_B \omega_{B,e}$$

and the value for α_B is 0.005 in the results presented here. This modified electron momentum transfer frequency is then used in the classical description of the transverse magnetic field electron mobility:

$$\mu_e = \frac{e}{m\nu_{mom}} \frac{1}{1 + \left(\frac{\omega_{B,e}}{\nu_{mom}} \right)^2}$$

Heavy Particle Behavior

To calculate both neutral depletion and ground state ionization, an MCC model is used. First, a probability of collision, P_C (generally <<1) is calculated as follows:

$$P_C^{neutral} = n_e k_i \Delta t$$

Then, at every timestep, each neutral macroparticle is assigned a random number from 0 to 1. If this random number is less than P_C, then a collision event is simulated and the neutral is changed to an ion. A collision

probability multiplier technique which permits partial ionization of the neutral macroparticles is used to ensure that sufficient ion macroparticles are generated for acceptable ion statistics. Ionization rates are taken from Garrigues et al.[xi]

The motion of the heavy particles is based on a first order advection scheme. Macroparticle are considered collisionless while positions and velocities are evaluated using a classical leapfrog update scheme. Neutrals are injected at the anode to match the desired mass flow rate and are removed from the simulation due to ionization. Xe^+ particles are generated by ionization with the properties of their parent neutral macroparticle. Wall recombination occurs when ions strike any thruster wall and results in the formation of an equal number of fully accommodated (1000 K) neutral particles. Neutral scattering at the wall is also based on full thermal accommodation.

Electron Energy

Electrons are assumed to be isothermal with a Maxwellian energy distribution along magnetic field lines. This allows for a 1-D decomposition of the electron energy equation across field lines. The complete electron energy equation is as follows:

$$\frac{\partial}{\partial t}\left(n_e \varepsilon\right) + \vec{\nabla} \bullet \left[\frac{5}{3} n_e \varepsilon \vec{u}_e - \frac{10}{9} n_e \mu_e \varepsilon \vec{\nabla} \varepsilon\right] = -n_e \vec{u}_e \bullet \vec{E} - n_e \varepsilon \nu_{loss}(\varepsilon)$$

The electron energy equation above can be recast in the form of an ordinary differential equation with a dependence on the electron energy alone. Stable integration of the resulting ODE requires a timestep far smaller than the timestep used for heavy particle evolution. As suggested by Fife[v], the electron energy equation is subcycled 100 times for every single heavy particle timestep to ensure accurate integration.

The active domain simulated by the electron energy equation is the same as for the potential calculation (between the VAL and the VCL). The electron energy between the VCL and domain exit is fixed at 2 eV while the electron energy in the Anode region is also fixed at a constant (chosen for this paper between 1-3 eV).

Computational Details

The computational model is compiled with SUN f90 to run on a SunBlade-1500 workstation. A simulation typically contains 100,000 ion macroparticles and 200,000 neutral macroparticles. The heavy particle timestep is limited to the time needed for a perfectly accelerated particle to cross a computational cell (which results in a timestep of about 5.0×10^{-8} seconds). Typical solution time is 12 hours.

IV. Anode Region Model

The anode region model used in this paper is based on the idea that the potential field in the Anode region must support a stable sheath on the interior surfaces of the thruster. To model this region, the generalized analytic Bohm criterion is used to evaluate the ion distribution function at the anode. If this criteria is not met, then this indicates that some correction must be made to the potential. Appropriate corrections to the potential are made and, over time, the simulations evolve towards the equilibrium potential configuration.

1. Generalized Analytic Bohm Criterion

The generalized analytic Bohm criterion, as developed by Chen[xii], can be written as:

$$\int_0^\infty \frac{g(v)}{v^2} dv \le \frac{M}{k_B T_e}$$

The ion distribution is constructed cumulatively (i.e. it reflects the contribution of all the ions which have reached the sheath edge during the entire simulation.) The use of this cumulative ion distribution function is justified by the

expectation that the anode region potential drop should eventually reach a steady configuration. In addition, particle statistics improve and statistical noise diminishes as new ions accumulate in the distribution function.

The generalized analytic Bohm criterion is evaluated across the entire anode face (labeled "Anode") as shown in Fig. 2.

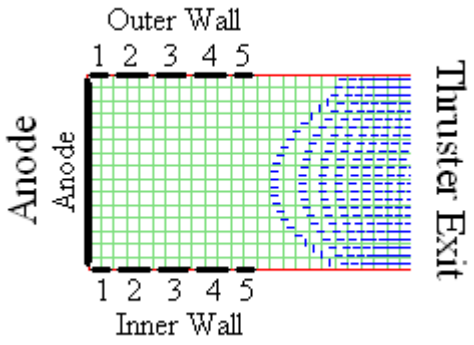

Figure 2. Anode Region Schematic

First dashed blue line from the left represents the VAL

To construct a 1-D anode region model, only the ion distribution anode segment is used to evaluate the Bohm criterion. This correction is added to the thermalized potential by raising the value of the VAL from the nominal 275 V to a corrected value (on the order of 285 V) while the anode is held at the nominal 275 V value and the VCL remains static at 0 V. The centerline thermalized potential is then linearly interpolated between the anode and the VAL to complete the 1-D centerline thermalized potential in the Anode region. Finally, the centerline thermalized potential is extrapolated along magnetic field lines (in exactly the same way as in the Hall region) to recover the full 2-D potential.

Proportional Feedback Controller

Implementation of the potential correction is achieved through the use of a simple proportional feedback controller. An error signal is developed from the discrepancy between the left and right hand side of the generalized analytic Bohm criterion formula. From this discrepancy, a baseline correction to the VAL potential is calculated. This baseline correction is multiplied by a proportional gain factor and is then applied to the VAL. Finally, changes to the VAL potential are updated only at prescribed intervals to account for the phase lag corresponding to the transit time of the ions from the VAL to the sheath edge.

Tuning of the controller involved the following adjustments:

- Varying the proportional gain factor
- Use of asymmetric gain factors
- Varying the phase lag of the controller

Despite expectation of full steady-state equilibrium convergence, only approximate convergence to various oscillatory solutions was observed. Nonetheless, the mean potential correction was consistent independent of the controller parameters. Therefore, it is believed that this proportional feedback controller provides the correct mean equilibrium potential correction; however, further work is necessary to develop a sufficient control scheme to minimize this oscillatory behavior.

V. Results and Discussion

The baseline simulation conditions with no anode region model are presented in Table 1.

Xenon Mass Flow Rate	5 mg/s
Potential Drop (between VAL and VCL)	275 V
Anode Mean Electron Energy	3 eV
Thrust	71.77 mN

Table 1. Baseline Operating Condition (no anode region model)

In order to study the effects of the feedback controller, simulations are run without the use of the proportional feedback controller. Instead, the potential correction at the VAL is enforced as a constant (at 5 V, 10 V, 15 V, and 20 V). During the course of simulation, the components of the generalized analytic Bohm Criterion formula are recorded at each timestep. From these results, provided in Fig. 3, it is possible to evaluate the percentage of time that the generalized analytic Bohm criterion is satisfied for a given constant potential correction. These results are provided in Table 2.

Potential Correction	Bohm Criterion Satisfied	Bohm Criterion Not Satisfied
5 V	0.10 %	99.90 %
10 V	0.15 %	99.85 %
15 V	81.46 %	18.54 %
20 V	77.72 %	22.28 %

Table 2. Percentage of time for which generalized analytic Bohm criterion is satisfied

From these results, it is clear in order for the generalized analytic Bohm criterion to be satisfied, a finite potential correction is required; however, simply increasing the potential correction does not necessarily ensure a more stable sheath. Also, even for a constant potential correction, the signal received at the anode (proportional to the LHS of the generalized analytic Bohm criterion formula) is highly nonlinear and unsteady. These observations motivated the development of a satisfactory feedback controller to control the potential correction dynamically.

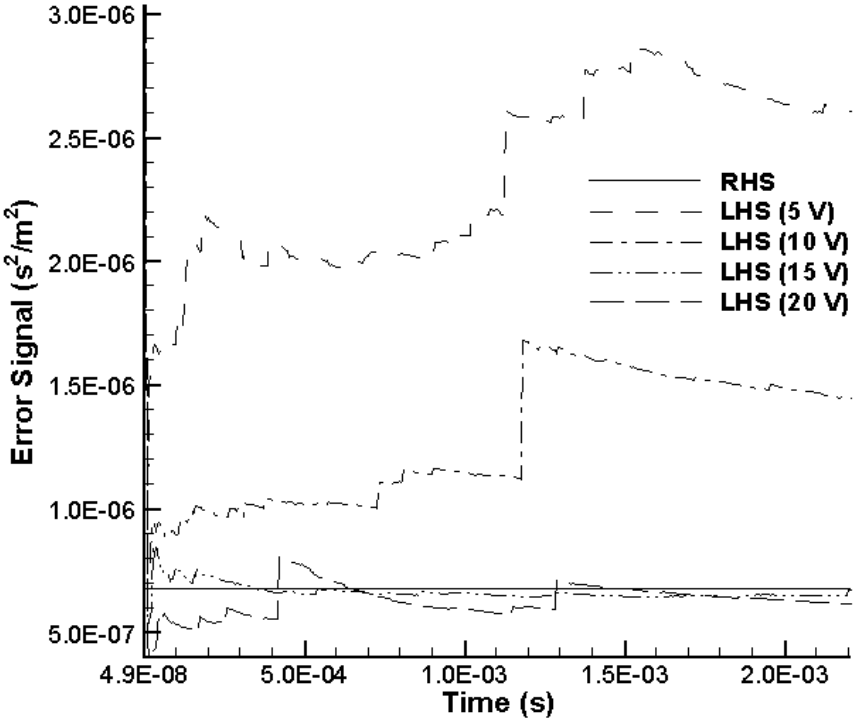

Figure 3. Left hand side (LHS) and right hand side (RHS) of the generalized analytic bohm formula for selected cases of constant potential correction at VAL. Note: Stable sheath exists when LHS is less than RHS**.**

To assess the proportional feedback controller performance, it is tuned on the baseline simulation. Various gains and phase lags are simulated and selected results are presented in Fig. 4. The statistics collected from these simulations are presented in Table 3.

Proportional Gain	Phase Lag (μs)	Mean (V)	Standard Deviation (V)
0.25	1.225	16.10	3.91
0.15	1.225	15.20	2.27
0.05	1.225	14.91	5.49
1.00	4.900	16.55	4.39
1.00	6.125	15.92	5.36
1.00	7.350	14.96	2.09
1.00	8.575	15.69	5.58
1.00	9.800	15.50	5.98
Average VAL Potential Conditions		15.60	4.38

Table 3. VAL Potential Correction for selected Feedback Controller configurations

From these results, it is clear that the feedback controller cannot resolve a completely steady anode region potential configuration. Instead, there is rough convergence to oscillatory potential configurations with no preferred amplitude or frequency; however, it is possible to characterize the VAL potential correction from the mean value of observed oscillatory VAL potential configurations.

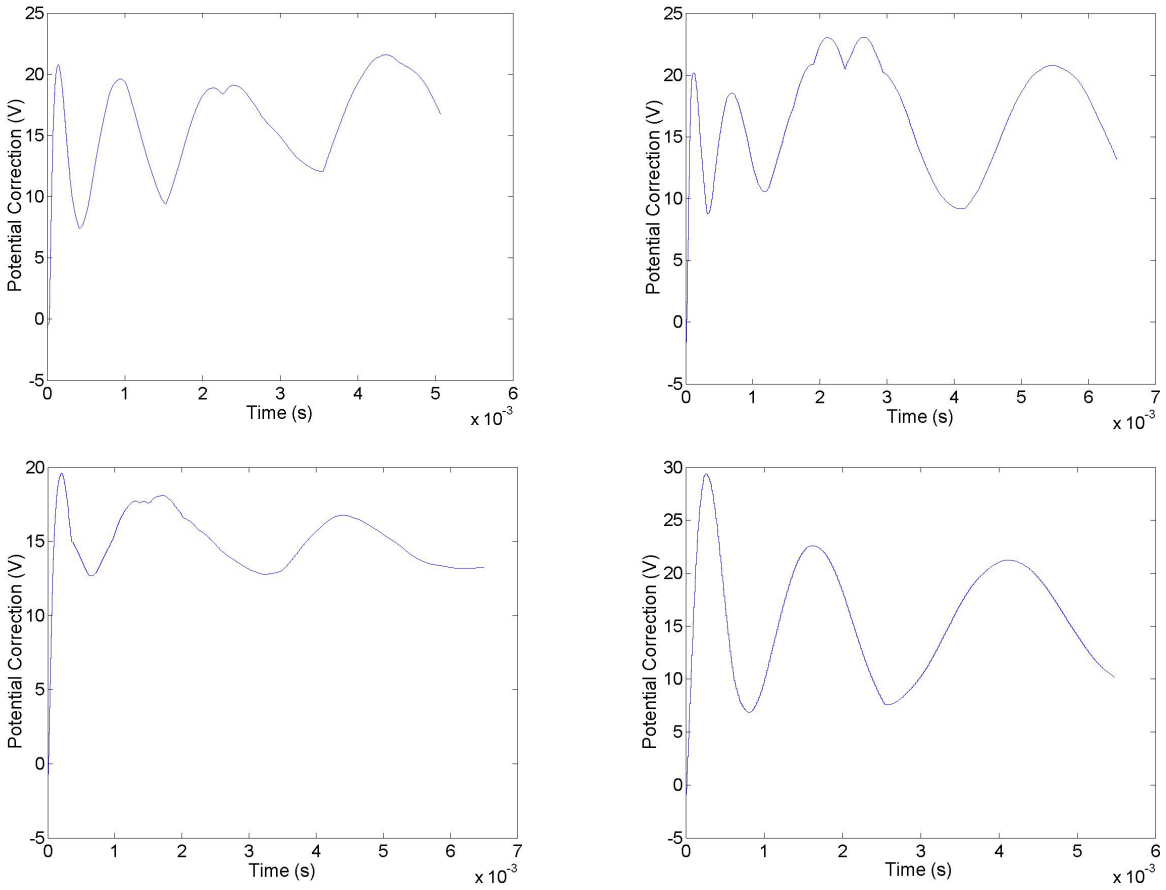

Figure 4. Selected potential correction from feedback controller. From upper left clockwise, (Proportional Gain - 0.25, Phase Lag – 1.225 μs), (Proportional Gain - 1.0, Phase Lag – 4.9 μs) , (Proportional Gain - 1.0, Phase Lag – 8.575 μs) , (Proportional Gain - 1.0, Phase Lag – 7.35 μs)

Simulations are run representing two particular anode electron energy cases (1 eV and 3eV) and the baseline case (no anode region model). The resulting performance parameters and mean value of the VAL potential correction are presented in Table 4. From these results it can be concluded that the inclusion of an anode model marginally diminishes the thrust produced by these simulations. The magnitude of the mean potential corrections is roughly between four and five times the magnitude of the anode electron energy; nonetheless, it must be noted that in these simulations, the heavy species are considered to be collisionless. Since collision driven pressure gradients are a physical mechanism known to contribute to the formation of a stable presheath, it is believed that the mean potential corrections listed in Table 4 represent the upper limit of expected potential correction to the anode region model.

Anode Energy (eV)	Anode Model	Thrust (mN)	Ion Current (A)	Mean Potential Correction (V)
3	No	71.77	3.665	N/A
3	Yes	68.87	3.652	15.18
1	Yes	67.11	3.678	4.05

Table 4. Performance Parameters for Baseline and Anode Model Cases

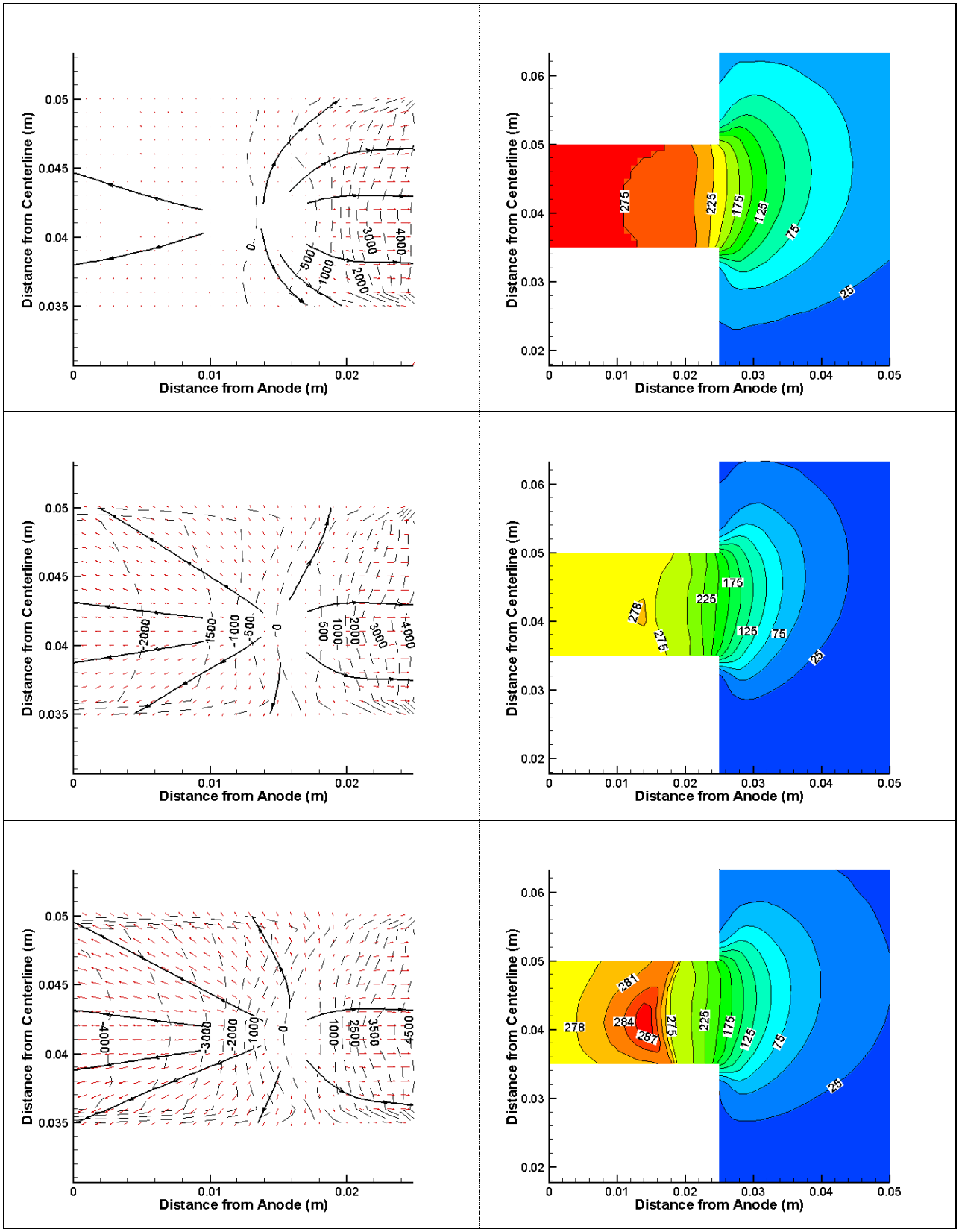

Figure 5. Mean Ion Velocity Vectors and Mean Axial Velocity Contours (Left Column) and Mean Potential (Right Column) From top to bottom: no anode model w/ 3 eV anode electron energy, anode model w/ 1 eV anode electron energy, anode model w/ 3 eV anode electron energy

Mean ion velocity vectors, mean axial velocity contours, and mean potential contours are presented in Fig. 5. The direct impact of the anode region model is the formation of a high voltage peak on the thruster centerline near the VAL. The anode region model changes the curvature of the zero axial velocity line and pushes it away from the anode. This effectively traps more ions in the backflux towards the anode. Since the 3 eV anode electron energy condition results in a higher potential correction, more ions are captured by the anode walls. This is especially evident in the streamtraces in Fig. 5. Finally, the magnitude of the axial velocity contours scales correctly with the anode electron energy (proportional to the square root of the energy).

Finally, the baseline simulation with potential correction is compared with a similar simulation that does not permit ionization upstream of the VAL. (This represents a case with no ionization near the anode.) The mean plasma densities for these two cases are represented in Fig. 6. The resulting mean potential corrections are 15.18 V for the case with ionization in the anode region and 11.55 V for the case with no ionization in the anode region. This result is expected because if ionization processes take place between the VAL and the anode, an additional potential correction must be applied to accelerate these new ions to the requisite velocity to maintain a stable sheath.

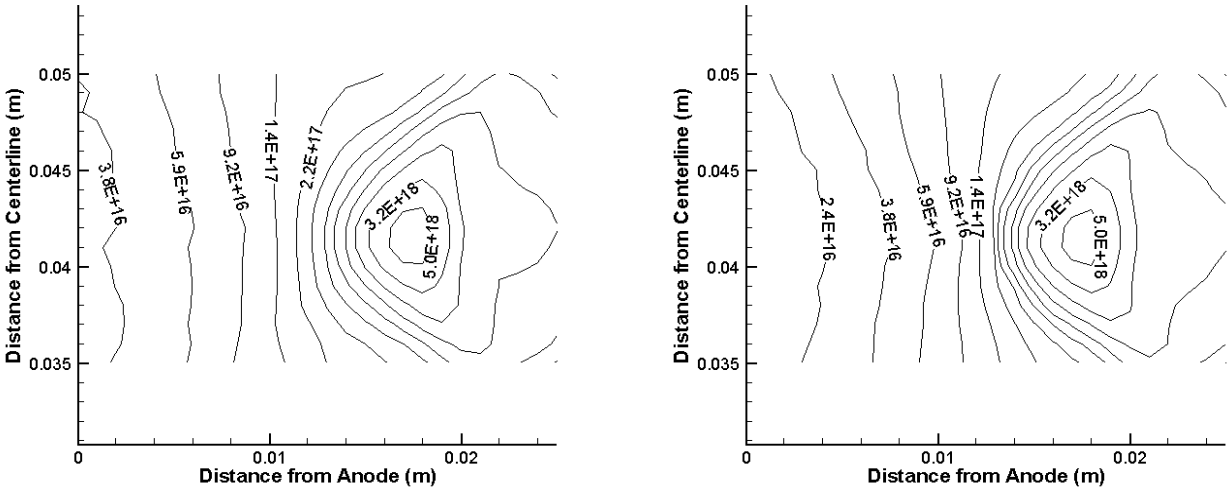

Figure 6. Mean Plasma Density (#/m^3)
Left Plot: Ionization near Anode; Right Plot: No Ionization near Anode

VI. Conclusions

A 2-D axisymmetric hybrid PIC-MCC model has been coupled with a 1-D anode region model. The linear feedback controller which was developed to implement this model proved to be only partially successful. It could achieve only rough convergence to an oscillatory potential configuration; however, this was sufficient to characterize the anode region potential drop from the mean value of the observed oscillatory solutions. Based on the results presented in this paper, the maximum expected anode region voltage drop is expected to be in the range of 4-5 times the anode electron energy. Also, inclusion of ionization in the region of the anode necessitates a larger potential drop in the anode region to maintain sheath stability. Finally, the correction to boundary conditions in the Hall region from the anode model results in slightly diminished thruster performance.

Many parameters used in this paper are not investigated in depth. First, the location of the VAL is fixed for all the results presented in this paper. This choice of this location is not completely arbitrary for the zero axial velocity line coincides relatively well with the VAL; however, due to the unsteady nature of the Hall region, it is likely that the zero axial velocity line in the thruster is not stationary. In addition, the use of linear interpolation to describe the shape of the anode region potential drop is largely motivated by the ease of implementation rather than strictly physical concerns. Finally, the validity of using the thermalized potential to extrapolate to the regular potential in the region near the anode is unclear.

In an effort to eliminate the oscillatory behavior observed in the potential correction convergence, the development of a more sophisticated PID controller is planned. As part of this effort, a more systematic identification of the anode region model system characteristics is necessary to develop this real-time controller. Finally, collisions must be included if the anode presheath is to be resolved correctly.

VII. Acknowledgements

The first author gratefully acknowledges financial support from the Department of Energy through a Computational Science Graduate Fellowship and from the University of Michigan through a Rackham Travel Fellowship. The first author also gratefully acknowledges the invaluable assistance provided by fellow graduate student Robert Bryant Lobbia.

---

[i] Keidar, M., Boyd, I.D., and Beilis, I.I., "Plasma Flow and Plasma-Wall Transition in Hall Thruster Channel," *Physics of Plasmas*, Vol. 9, 2002, pp. 5315-5322.

[ii] Ahedo, E., Martinez-Cerezo, P., and Martinez-Sanchez, M., "One-Dimensional Model of the Plasma Flow in a Hall Thruster," *Physics of Plasmas*, Vol. 8, 2001, pp. 3058-3068.

[iii] Roy, S. and Pandey, B.P., "Numerical investigation of a Hall thruster plasma", *Physics of Plasmas*, Vol. 9, 2002, pp. 4052-4060.

[iv] Komurasaki, K. and Arakawa, Y., "Two-Dimensional Numerical Model of a Plasma Flow in a Hall Thruster," *Journal of Propulsion and Power*, Vol. 11, 1995, pp. 1317-1323.

[v] Fife, J.M., "Hybrid-PIC Modeling and Electrostatic Probe Survey of Hall Thrusters," Doctoral Thesis, Massachusetts Institute of Technology, Department of Aeronautics and Astronautics, September 1998.

[vi] Boeuf, J.-P. and Garrigues, L., "Low Frequency Oscillations In a Stationary Plasma Thruster," *Journal of Applied Physics*, Vol. 84, 1998, pp. 3541-3544.

[vii] Hagelaar, G. J. M., Bareilles, J., Garrigues, L., and Boeuf, J.-P., "Two-dimensional model of a stationary plasma thruster," *Journal of Applied Physics*, Vol. 91, 2002, pp.5592-5598.

[viii] Keidar, M., Boyd, I. D. and Beilis, I. I., Analysis of the anode region of a Hall thruster channel, AIAA-2002-4107, July 2002.

[ix] Koo, J. W., Boyd, I. D., "Computational Modeling of Stationary Plasma Thrusters." AIAA-2003-10113, July 2003.

[x] Morozov, A. I., Esipchuk, Yu. V., Tilinin, G. N., Trofimov, A. V., Sharov, Yu. A., Shchepkin, G. Ya., "Plasma Accelerator With Closed Electron Drift and Extended Acceleration Zone," *Soviet Journal of Plasma Physics*, Vol. 17, 1972, p.38.

[xi] Garrigues, L., Boyd, I.D., Boeuf, J.P., "Computation of Hall Thruster Performance," *Journal of Propulsion and Power*, Vol. 17, 2001, pp. 772-779.

[xii] Chen, F.F., *Phys. Fluids*, Vol. 25, 1982, p. 2385.